Lower hybrid plasma heating in a magnetic-mirror field

C. da C. Rapozo, A. S. de Assis, A. Serbêto, and L. T. Carneiro
Instituto de Física, Universidade Federal Fluminense, 24.020 Niterói, Rio de Janeiro, Brazil
(Received 1 October 1991)

The plasma heating by radio-frequency (rf) waves in the lower hybrid range of frequency has been studied using Langmuir and magnetic probes and also a Faraday cup. The plasma was confined in a mirror magnetic structure called LISA. It has been shown that the plasma heating rate depends on the resonant volume created by the ambient magnetic field. Also, the plasma potential drops due to the presence of the rf wave. The plasma we have considered was weakly ionized ($<1\%$) due to the presence of a 28-MHz rf source. The quality factor of the machine is comparable to the lower hybrid Landau one.

PACS number(s): 52.50.Gj, 52.55.Jd

I. INTRODUCTION

The interaction of rf radiation with plasmas has been studied for several decades in fusion and space plasmas. However, many features of those interactions are still open to investigation. We can mention the influence on the plasma potential that is of paramount importance as far the impurity control is concerned and also the effect of the ambient magnetic geometry on rf power absorption, which is very important not only in nuclear fusion but also in space plasma physics where the ambient magnetic-field geometry (in general almost dipolar) is very complex. In this paper we present some experimental results we have obtained in a LISA mirror magnetic-field device, as shown in Fig. 1 and Table 1, on the two above-mentioned problems [1].

II. EXPERIMENTAL RESULTS AND ANALYSIS

Starting this investigation, we consider the lower hybrid resonance effect on the plasma potential when the resonant volume size is changed in a helium plasma. It was created in the metallic cylindrical vessel of the mirror linear device LISA. The rf source built at UFF uses a 28-MHz and 50-W injected power and an oscillator (Toshiba Model No. 6F50RA). The lower hybrid wave launched into the plasma was generated by a helicoidal antenna with an inner radius of 5 cm and a length of 22 cm. The rf breakdown system occurs for 0.8 V/cm. The temperature and plasma density are obtained by a cylindrical disk plane Langmuir probe. We also use a Faraday cup to measure the electron and ion temperature to check the Langmuir probe measurements. The electric fields of the wave E_r, E_θ, and E_z are measured by a double floating electrostatic probe. The static magnetic field is measured by a Hall probe. At $r=\pm 5$ cm the wave needs to go through this layer to reach the plasma center and the rf wave obeys the accessibility condition [2–4]

$$n_z^2 \geq 1+\omega_{pe}^2/\omega_{ce}^2|_{\omega=\omega_{\mathrm{LH}}} . \tag{1}$$

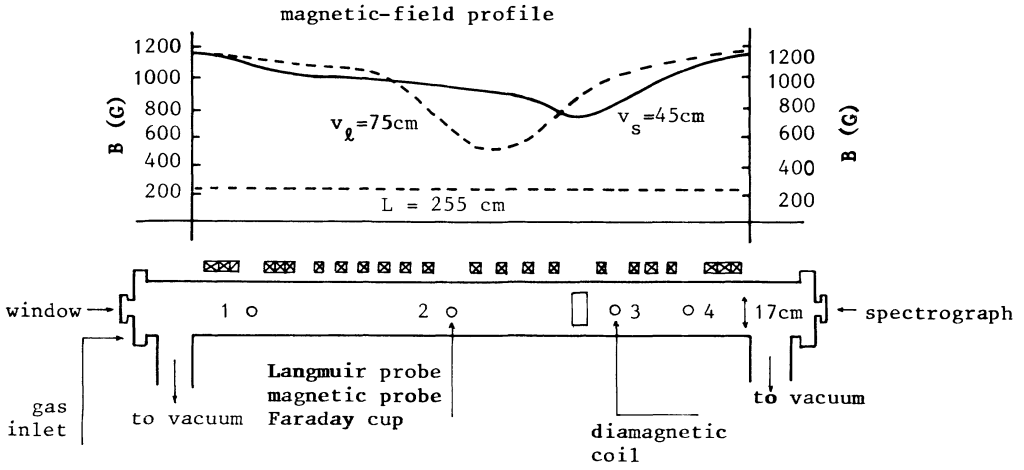

FIG. 1. Dimensions of the linear mirror machine LISA and the experimental arrangement plus the axial distribution of the equilibrium magnetic field.

TABLE I. Summary of the basic LISA and target plasma parameters.

Total length L	255 cm
Inner radius r	8.5 cm
Uniform magnetic field B	10.5 kG
Mirror region B	13.0 kG
Extension of the uniform magnetic field	100 cm
Electron density n_e	10^{10} cm^{-3}
Electron temperature T_e	80 eV
Ion temperature T_i	10 eV

The lower hybrid layer is identified experimentally observing the $K_\perp$ value that reaches its maximum at $r=\pm 5$ cm characterized by a temperature rise. Landau damping is responsible for wave dissipation. The wave vector from the cold plasma dispersion relation has its imaginary part increased, with the largest part of dissipation taking place at $r=\pm 5$ cm, the hybrid layer. Figure 2 shows the profiles of the parallel electron temperature $T_{e\parallel}$ for two different resonant volume sizes, namely, the large and small resonant volumes. We operate with seven disconnected coils next to the waveguide port to get a large resonant volume and a better confinement. To get a small resonant volume, four disconnected coils are used. The peaks in the temperature profile show that the rf energy is thermalized close to the lower hybrid layer.

When the resonant lower hybrid layer is reached, which is accessible from the low-density side which requires [5]

$$n_z^2 \geq 1+(\omega_{pe}^2/\omega_{ce}^2)|_{\omega=\omega_{\mathrm{LH}}} ,$$

the E_r, E_θ, and E_z profiles are modified by the resonant absorption; the rf frequency condition $f_{\mathrm{rf}}=f_{\mathrm{LH}}$ has to be satisfied. Figures 3(a), 3(b), and 3(c) show the experimental data of the field profiles in the case of $4<r<5$ cm, which have an abrupt drop. This can be understood as follows: As $K_\perp$ increases, then $E_z \cong AJ_0(\mathbf{K}_\perp \cdot \mathbf{r})$ and $E_\theta \cong AJ_1(\mathbf{K}_\perp \cdot \mathbf{r})$ decrease abruptly outside of the layer. $\mathbf{K}_\perp$ has typical values of $0.5<K_\perp<1.0$ cm^{-1}. Nevertheless, near the column axis the electric fields ($r<5.0$ cm) have Bessel's-function dependence. The field E_θ has a minimum value in the axis and E_z has a maximum one.

Using $K_\parallel \simeq 2.0$ cm^{-1}, 4.0 cm^{-1}, 8.0 cm^{-1}, etc., da C. Rapozo *et al.* [2] show that in the resonant layer the field **E** of the plasma has a minimum, similar to the plasma potential drop.

Figure 4 shows a dip of the plasma potential localized in the points $r=\pm 5.0$ cm for the large resonant volume and small resonant volume, respectively, for the same frequency.

The drop of the plasma potential as a function of the magnetic field is the same as in the case of the anomalous diffusion for dc discharges in a magnetic field [6,7]. In dc discharges the instability appears in the plasma column. This instability causes a modification of the particle diffusion in the parallel and perpendicular directions to the magnetic field. Plasmas produced by rf do not have the same currents as in dc plasma discharges.

The dependence of the plasma potential V_p with the magnetic field, and the electric field components E_θ and E_r of the wave, can be seen in Figs. 3(a) and 3(b). The values of these fields are larger for the small resonant volume, since these fields are related to the perpendicular velocity $v_\perp$ through the expression

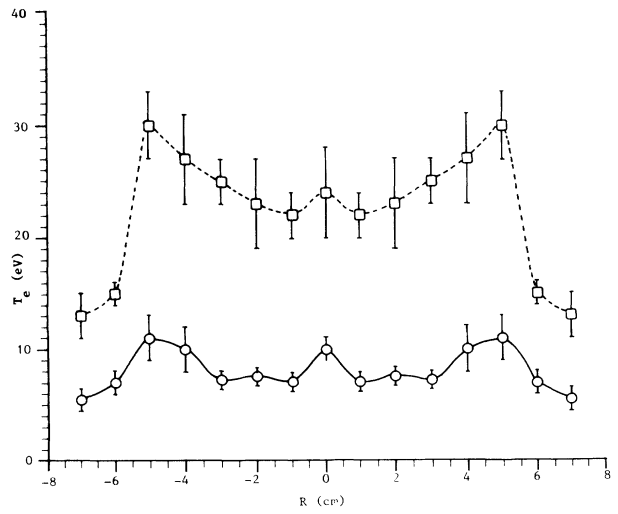

FIG. 2. Electron temperature profile vs radius for the large resonant volume (dashed line) and the small resonant volume (solid line).

$$v_\theta = \frac{eE_\theta}{m\omega_{\mathrm{rf}}} \tag{2}$$

and

$$v_r = \frac{eE_r}{m\omega_{\mathrm{rf}}} \tag{3}$$

such that $v_\perp$ can be written as

$$V_\perp = \sqrt{V_\theta^2 + V_r^2} \tag{4}$$

or redefined as

$$v_\perp = v_\parallel \sqrt{R_m - 1} , \tag{5}$$

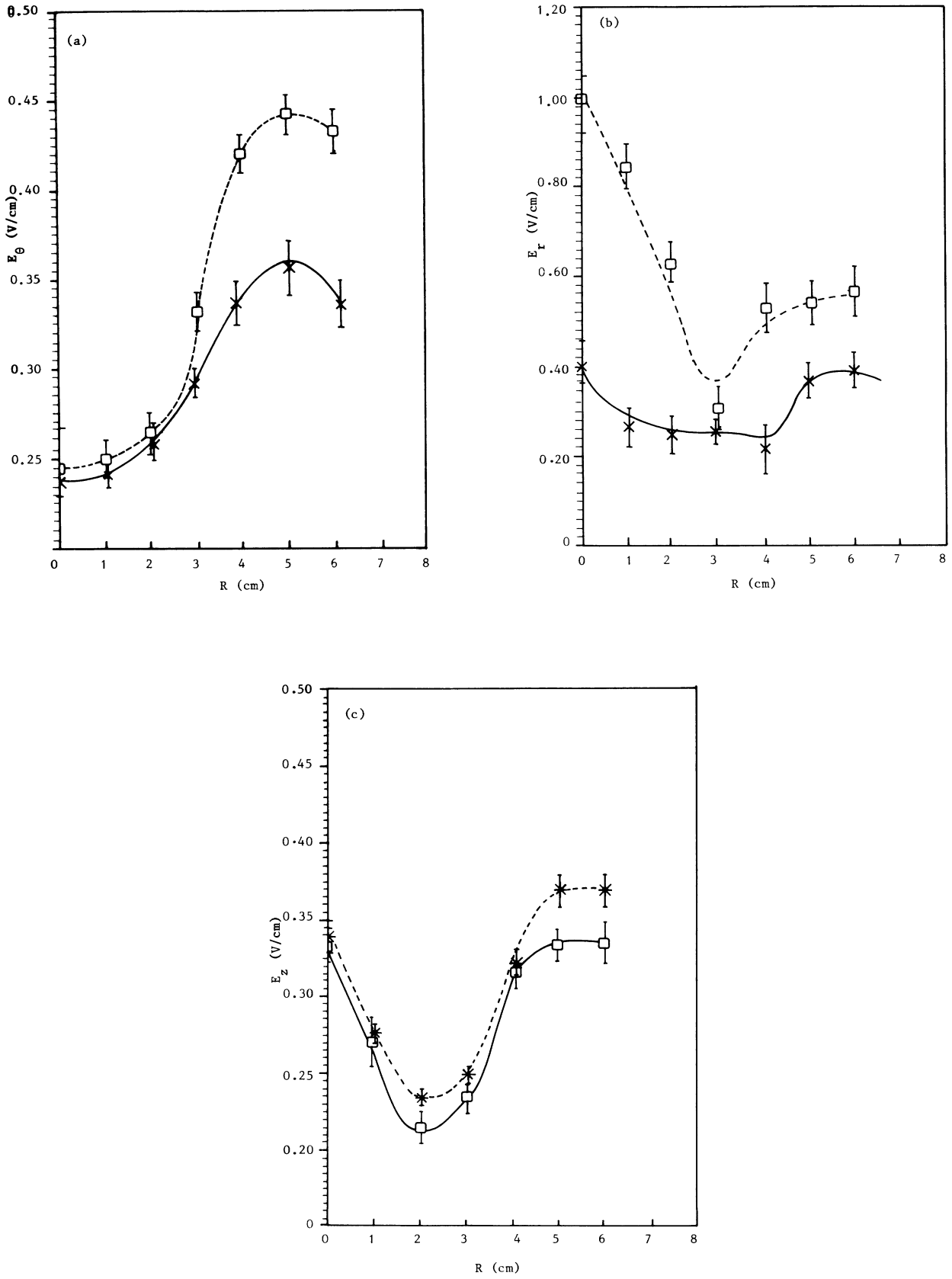

FIG. 3. (a) Electric field E_θ profile vs radius for the large resonant volume (solid line) and the small resonant volume (dashed line). (b) Electric field E_r profile vs radius for the large resonant volume (solid line) and the small resonant volume (dashed line). (c) Electric field E_z profile vs radius for the large resonant volume (dashed line) and the small resonant volume (solid line).

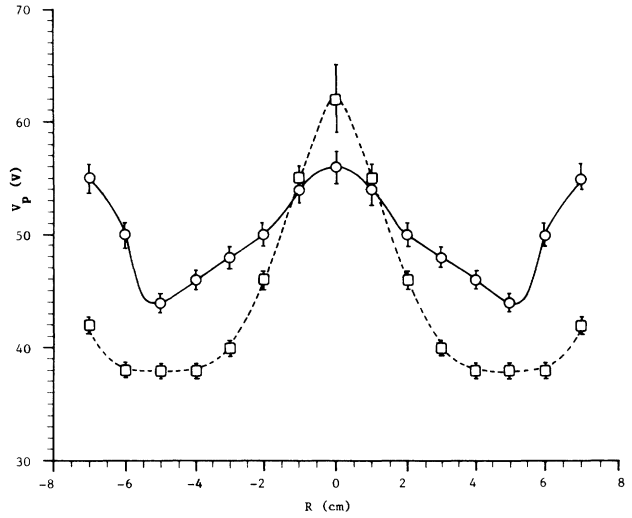

FIG. 4. Plasma potential profile vs radius for the large resonant volume (dashed line) and the small resonant volume (solid line).

where $v_{\parallel}$ is the parallel component of the velocity and R_m is the mirror ratio. The increasing of these fields is due to the interaction of the rf wave with the electrons contained in the small resonant volume; as a consequence, the perpendicular electric field $\mathbf{E}_{\perp}$ also increases.

The parallel component of the electric field is given by

$$E_{\parallel} = -(D_{\parallel}^{e}/\mu_e)(\nabla n/n)Q_e \ , \tag{6}$$

where we have assumed that the confinement factor is

$$Q_e = 1-[\pi(R-r_{\perp})^2/\pi R^2][A/(A+B)] \ . \tag{7}$$

In this equation R is the LISA inner radius, and $r_{\perp}$ is the Larmor radius for electrons. A and B are, respectively, the density of electrons confined and not confined by the magnetic mirror, which are obtained by the following expressions:

$$A = G\int\int \exp[-a^2(v_{\parallel}^2+v_{\perp}^2)]2\pi v_{\perp}dv_{\perp}dv_{\parallel} \tag{8}$$

and

$$B = n_e - A \ , \tag{9}$$

where $n_e \approx 4.0\times 10^9$ cm^{-3} is the equilibrium electron plasma density. If we consider the isotropic temperature condition [8,9] $T_{\parallel}=T_{\perp}$, we have the A value and then obtain

$$\frac{A}{n_e} = \left[\frac{R_m-1}{R_m}\right]^{1/2} . \tag{10}$$

The percentage of particles lost in the mirror is 0.04 for the large resonant volume and 0.10 for the small resonant one. The perpendicular velocity given by the expression (5) is $V_{\perp}\approx 6.3\times 10^5$ cm/s for the large resonant volume and $V_{\perp}\cong 9.2\times 10^5$ cm/s for the small resonant one. These two values agree with the experimental results shown in Figs. 3(a) and 3(b). On the other hand, Eq. (10) shows that relation (7) is bigger than that of the large resonant volume; consequently, relation (6) is also bigger than that of the large resonant volume. This fact agrees with experimental data of the electric field E_z shown in Fig. 3(c). The effective increase of the electron temperature at $r=5.0$ is related to the large value of the perpendicular electric field $E_{\perp}=\sqrt{E_{\theta}^2+E_r^2}$. This fact shows that the wave absorption occurs at the wave region where the temperature increases. It means that the rf energy is thermalized efficiently close to the lower hybrid layer, as we have mentioned before. This can be understood since the wave quality factor is smaller than that of the LISA cavity for lower hybrid waves.

Figure 5 shows the modulus $E_{\theta}(|E_{\theta}|)$ for large (dashed line) and small (solid line) resonant volumes and $B_z(|B_z|)$ versus radius. The peak of E_{θ} occurs at $r=5.0$ cm. In the wall $E_{\theta}=0$, which in this case is not used because close to the wall the plasma is cold. These experimental data have a very good agreement with theory [2].

Figures 6(a) and 6(b) show the power deposition profile

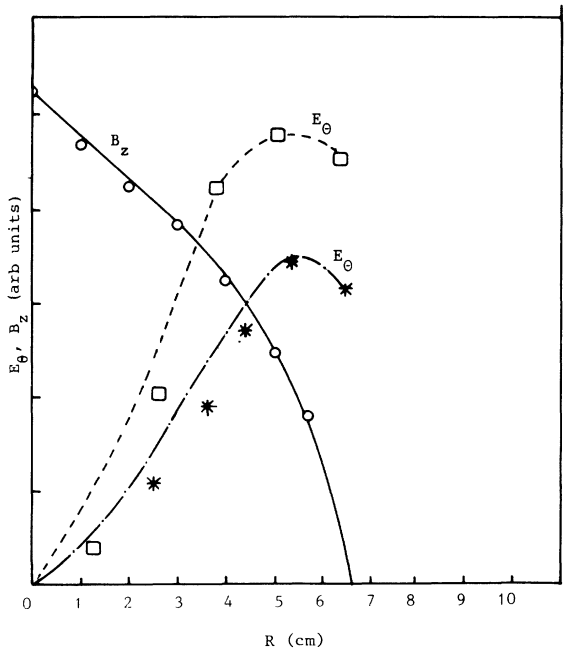

FIG. 5. Modulus of $E_{\theta}(|E_{\theta}|)$ and $B_z(|B_z|)$ profiles vs radius for the large resonant volume (solid line) and the small resonant volume (dashed line).

versus radius for the large resonant volume (dashed line) and the small resonant volume (solid line) for the cases without and with plasma; these data permit us to obtain the quality factor Q of the LISA cavity.

The plasma potential drops due to the lower hybrid heating. This fact is explained as a consequence of the increase of the ratio between the perpendicular and parallel temperatures at the lower hybrid resonance; the same effect occurs at the electron cyclotron resonance zone [9]. Figure 4 shows the plasma potential for both cases of the resonant volume sizes. In these cases we observe a potential drop at the region near $r = \pm 5.0$ cm, where the lower hybrid resonant layer is located.

III. CONCLUSION

In conclusion, we have shown that, in the LISA device, the rf wave of 28 MHz is absorbed because of the lower hybrid resonance. The rf energy is thermalized very close to the resonance layer due to Landau and collisional damping. As a consequence, we have identified a very clear plasma potential drop.

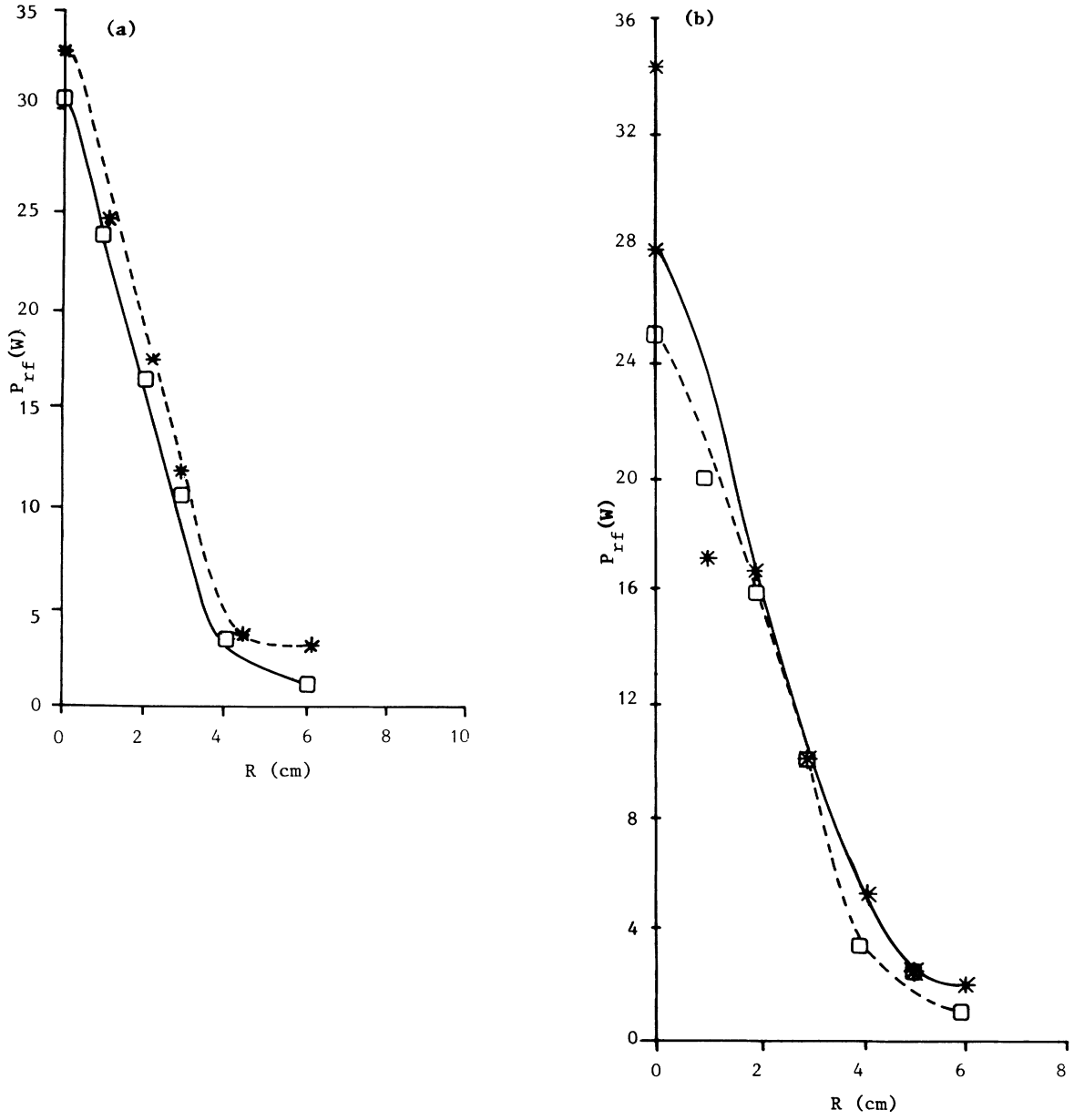

FIG. 6. (a) Power deposition profile vs radius, without plasma, for the large resonant volume (dashed line) and the small resonant volume (solid line). (b) Power deposition profile vs radius, with plasma, for the large resonant volume (dashed line) and the small resonant volume (solid line).

ACKNOWLEDGMENTS

The authors are grateful to N. L. P. Mansur, and the students R. P. Menezes and P. C. M. da Cruz (CNPq) for their contributions to this paper. This work was supported by CNPq (Conselho Nacional de Desenvolvimento Científico e Tecnológico) and FINEP (Financiadora de Estudos e Projetos) of Brazil.

[1] N. A. Krall and W. Trivelpiece, *Principles of Plasma Physics* (McGraw-Hill–Kolukusha, Tokyo, Japan, 1973).
[2] C. da C. Rapozo, J. C. X. da Silva, A. S. de Assis, R. Y. Honda, H. R. T. Silva, and P. H. Sakanaka, Plasma Phys. Controll. Fusion **30**, 1187 (1988).
[3] S. Kuhn, Phys. Fluids **24**, 1586 (1981).
[4] S. Kuhn, Phys. Fluids **27**, 1821 (1984).
[5] M. Kramer, Plasma Phys. **17**, 373 (1975).
[6] F. C. Hoh and B. Lehnert, Phys. Fluids **3**, 600 (1960).
[7] G. A. Paulikas and R. V. Pyle, Phys. Fluids **5**, 348 (1962).
[8] C. da C. Rapozo, A. S. de Assis, and J. Busnardo-Neto, Phys. Rev. A **42**, 989 (1990).
[9] C. da C. Rapozo, A. S. de Assis, and J. Busnardo-Neto, Plasma Phys. Controll. Fusion (1991).